Supplement of Atmos. Chem. Phys., 21, 14333–14349, 2021
https://doi.org/10.5194/acp-21-14333-2021-supplement

Atmospheric Chemistry and Physics
Open Access
EGU

Supplement of

Impact of pyruvic acid photolysis on acetaldehyde and peroxy radical formation in the boreal forest: theoretical calculations and model results

Philipp G. Eger et al.

Correspondence to: John N. Crowley (john.crowley@mpic.de)

Table S1 Summary of literature results for pyruvic acid photolysis at actinic wavelengths

	Vesley 1964 N_2 or O_2	Grosjean 1983 Air	Yamamoto 1985 Inert + O_2	Yamamoto 1985	Berges 1992 Air	Hjorth 2002 Moortgat 2001 [6] Air	Reed-Harris 2016 N_2	Reed-Harris 2017 N_2	Reed-Harris 2016 Air	Reed-Harris 2017 Air	Samanta 2021 He
λ (nm)	366	sunlight	366	345, 320	350	Sunlight	Solar-sim 290-380	Solar-sim 290-380	Solar-sim 290-380	Solar-sim 290-380	351
P (mbar)	67	1000	1.33-13.3		1000	1000	0-800	1000	0-800	1000	5.33
O_2 (mbar)	0 or 67	4.9e18			4.9e18	4.9e18	0	0	4.9e18	4.9e18 varied	0
T (K)	355 ± 3	Ambient	340	340	RT	Ambient	295	RT	295	RT	298
[PA]	~1e17	8e12			1.2-2.4e15	Not listed	9.7e15	7-29e13	9.7e15	7-29e13	1.5e14
ϕ (1 bar, in %)		62 [3]			85±16	43 or 28 [7]	~20 [9]	84±10	19 [8]	320±50	--
ϕ (P)	102 ± 6										$100^{0}_{0.4}$
Product yields (%)											
CO_2	100		90 ± 10 [13]		127±18	-- [7]	115±17	16±9	110 ± 25	108±19	97
CH_3CHO (AC)	60-65	6[2]	AC/CO_2 = 0.45	AC/CO_2 = 0.3-0.8 [12]	48±1	Main product	51±9	10±1	46 ± 11	5±2 [5]	AC/CO_2 = 0.34 ± 0.2 [11]
CH_2=CHOH (VA)	--	--	Na [14]	--	--	20-44% of CH_3CHO	--	--	--	--	VA/CO_2 = 0.16 ± 0.1 [11]
$CH_3C(O)OH$	--	--	--	--	14	29-65% of CH_3CHO	9±2	5±1	18 ± 6	63±12 [4]	--
PAN	--	9 [2]	--	--	15±2 [1]	--	--	--	--		--
CO	1-2	--			< 13	15-50% of CH_3CHO	3.5±0.5	0.6±0.3	3.4 ± 0.7	3±2	--
CH_3OH	--	--	--	--	< 4		14±3	--	4 ± 2	5±2	--
HCHO	--	31[2]	--	--	--	14-65% of CH_3CHO	--	--	--	8±2	--
HC(O)OH	--	--	--	--	--	6-40% of CH_3CHO	1.9±0.5	--	5 ± 2	--	--
CH_3COH	--	--	--	--	--	--	--	--	--	--	100 [10]
CH_3CO + HOCO	--	--	--	--	--	--	--	--	--	--	0^{0}_{-2}
R(CH_3COH+PA) s^{-1} [14]	--	80	--	--	12000-24000	--	97000	700-2900	97000	700-2900	1500
R(CH_3COH +O_2) s^{-1} [15]	--	~1	--	--	~1	~1	--	--	~1	~1	--

Notes:

The OH yield (≈ 5%) reported by Mellouki and Mu (351 nm) is not included as thermodynamic considerations suggest that this is unlikely to have been a single photon process.
RT = Room temperature

1. When NO_2 was added PAN was formed and CH_3CHO yield was reduced to 30±4 %
2. Calculated from Figure 2 in Grosjean et al. ΔHCHO = 94 ppb, ΔCH_3CHO = 17 ppb, ΔPA = 300 ppb. For experiments with NO_2, ΔPAN = 36 ppb, ΔPA = 400 ppb.
3. EMAC model used to calculate the actinic flux at the location and date. The loss rate of PA was corrected for the 95 % transmission of actinic flux of the chamber walls and converted to a quantum yield.
4. Effective yield calculated from the loss of PA via photolysis only (PA was lost through other processes in air).
5. The yield of CH_3CHO was gradually reduced as O_2 was added. At the same time, the yields of acetic acid, formaldehyde and methanol increased.
6. Data of Hjorth et al were reported in Calvert et al (2011).
7. Calvert et al (2011) calculated actinic flux at the Euphore chamber to convert decay rate constants to a quantum yield and derived $\phi = 0.28$. We also list the quantum yield of 0.43 reported by Moortgat et al (2001) for the same chamber and analysis. CO_2 was observed but a high background in the chamber prevented quantitative analysis.
8. Based on Reed Harris et al. Data in air with 0.3 Torr PA. The value at 1000 mbar is an extrapolation of a fit to their data between 0 and 600 Torr, with a correction to reduce ϕ to 1 at zero pressure. Note that Reed Harris et al. used the UV-cross-sections evaluated by NASA, which are a factor 1.1 larger than IUPAC recommend. This implies that their values of ϕ must also be increased by this factor.
9. The value obtained in N_2 at 600 Torr was slightly larger (8%) than in air at the same pressure.
10. The measured yield of thermalised CH_3COH is 0.5 which was derived from the yield of CO_2 minus the combined yields of CH_3CHO and CH_2=CHOH. The initial yield of CH_3COH is 1 (like CO_2) but this has enough internal energy to isomerise before it is detected.
11. Calculated from $(AC+VA)/CO_2 = 0.5 \pm 0.3$ and $AC/VA = 2.1 \pm 0.4$
12. Yields at 345 and 320 nm were time dependent, hence the large range of values. The CH_3CHO/CO_2 ratio decreased with added air (~0.65 at zero air, ~0.1 at 150 Torr air).
13. Not affected when adding 160 Torr air.
14. CH_2=CHOH was not measured but was suggested to have been present to explain the reduction in CH_3CHO yield when adding air.
15. Based on a rate coefficient of 3×10^{-19} cm^3 $molecule^{-1}$ s^{-1} for $CH_3COH + O_2$.
16. Based on a rate coefficient of 1×10^{-11} cm^3 $molecule^{-1}$ s^{-1} for CH_3COH + pyruvic acid.

Vesley 1964 = Vesley, G. F., and Leermakers, P. A.: Photochemistry of alpha-keto acids + alpha-keto esters. 3. photolysis of pyruvic acid in vapor phase, J. Phys. Chem., 68, 2364-2366, doi:10.1021/j100790a507, 1964.
Grosjean 1983 = Grosjean, D.: Atmospheric reactions of pyruvic-acid, Atmos. Env., 17, 2379-2382, doi:10.1016/0004-6981(83)90242-1, 1983.
Yamamoto 1985 = Yamamoto, S., and Back, R. A.: The photolysis and thermal-decomposition of pyruvic-acid in the gas-phase, Can. J. Chem., 63, 549-554, doi:10.1139/v85-089, 1985.
Berges 1992 = Berges, M. G. M., and Warneck, P.: Product quantum yields for the 350 nm photodecomposition of pyruvic-acid in air, Berichte Der Bunsen-Gesellschaft-Physical Chemistry Chemical Physics, 96, 413-416, doi:10.1002/bbpc.19920960334, 1992.
Moortgat 2001 = Moortgat, G. K.: Important photochemical processes in the atmosphere, Pure Appl. Chem., 73, 487-490, doi:10.1351/pac200173030487, 2001.
Reed-Harris 2016 = Reed Harris, A. E., Doussin, J. F., Carpenter, B. K., and Vaida, V.: Gas-Phase Photolysis of Pyruvic Acid: The Effect of Pressure on Reaction Rates and Products, J. Phys. Chem. A, 120, 10123-10133, doi:10.1021/acs.jpca.6b09058, 2016.
Reed-Harris 2017 = Reed Harris, A. E., Cazaunau, M., Gratien, A., Pangui, E., Doussin, J.-F., and Vaida, V.: Atmospheric Simulation Chamber Studies of the Gas-Phase Photolysis of Pyruvic Acid, J. Phys. Chem. A, 121, 8348-8358, doi:10.1021/acs.jpca.7b05139, 2017.
Samanta 2021 = Samanta, B. R., Fernando, R., Rösch, D., Reisler, H., and Osborn, D. L.: Primary photodissociation mechanisms of pyruvic acid on S1: observation of methylhydroxycarbene and its chemical reaction in the gas phase, Phys. Chem. Chem. Phys., 23, 4107-4119, doi:10.1039/D0CP06424F, 2021.

Table S2: Overview of instruments and measured parameters in the IBAIRN campaign.

Measurement	Technique	Resolution[a]	LOD[b]	Uncertainty	References
Pyruvic acid	CI-QMS	10 s	15 pptv	30 %	Eger et al. (2020)
NO	CLD	5 s	5 pptv	20 %	Liebmann et al. (2018)
NO_2	TD-CRDS	60 s	60 pptv	6 %	Sobanski et al. (2016)
ΣPNs	TD-CRDS	60 s	60 pptv	6 %	Sobanski et al. (2016)
O_3	UV	10 s	~ 1 ppbv	2 %	Eger et al. (2020)
CO	QCL			20 %	Eger et al. (2020)
Monoterpenes (sum)	PTR-MS	10 min	5pptv		Liebmann et al. (2018)
Monoterpenes (speciated)	GC-AED	60 min	1 pptv	10 %	Liebmann et al. (2018)
HC(O)OH, $CH_3C(O)OH$, $CH_3C(O)C_2H_5$, MVK	PTR-MS tower[c]	30 min	--	--	
UVB-radiation	Solar Rad.				Petäjä et al. (2009)
Photolysis rates	Spectral Radiometer	10 s		15 %	Meusel et al. (2016)
BL height	LIDAR				Hellén et al. (2018)

CI-QMS = Chemical Ionisation Quadrupole Mass Spectrometer; CLD = Chemiluminescence detector; TD-CRD = Thermal Dissociation Cavity Ring-down Spectroscopy; I-CIMS = Iodide Chemical Ionisation Mass Spectrometer; UV = UV absorption spectroscopy; QCL = Quantum Cascade Laser absorption spectrometer; PTR-MS = Proton Transfer Reaction Mass Spectrometer; GC-MS = Gas Chromatography Mass Spectrometer; AED = Atomic Emission Detector; LOPAP = Long Path Absorption Photometer; CIMS = Chemical Ionisation Mass Spectrometry; Solar Rad. = Solar Radiometer (data provided via SmartSMEAR, Junninen et al. (2009)); Radiometer = Spectral radiometer. [a]Res = Time resolution; [b]LOD = Limit of detection, at the time resolution of the corresponding instrument. PTR-MS (*m/z* 47, 61, 71 and 73) sampling at different heights from a tower. Data at 42, 84, 168 and 336 m were averaged to generate a diel-profile.

Eger et al. 2020 = Eger, P. G., Schuladen, J., Sobanski, N., Fischer, H., Karu, E., Williams, J., Riva, M., Zha, Q., Ehn, M., Quéléver, L. L. J., Schallhart, S., Lelieveld, J., and Crowley, J. N.: Pyruvic acid in the boreal forest: gas-phase mixing ratios and impact on radical chemistry, Atmos. Chem. Phys., 20, 3697-3711, doi:10.5194/acp-20-3697-2020, 2020.

Liebmann et al. 2018 = Liebmann, J., Karu, E., Sobanski, N., Schuladen, J., Ehn, M., Schallhart, S., Quéléver, L., Hellen, H., Hakola, H., Hoffmann, T., Williams, J., Fischer, H., Lelieveld, J., and Crowley, J. N.: Direct measurement of NO_3 radical reactivity in a boreal forest, Atmos. Chem. Phys., 2018, 3799-3815, doi:10.5194/acp-18-3799-2018, 2018.

Sobanski et al. 2016 = Sobanski, N., Schuladen, J., Schuster, G., Lelieveld, J., and Crowley, J. N.: A five-channel cavity ring-down spectrometer for the detection of NO_2, NO_3, N_2O_5, total peroxy nitrates and total alkyl nitrates, Atmos. Meas. Tech., 9, 5103-5118, doi:10.5194/amt-9-5103-2016, 2016.

Petäjä et al. 2009 = Petäjä, T., Mauldin, I. R. L., Kosciuch, E., McGrath, J., Nieminen, T., Paasonen, P., Boy, M., Adamov, A., Kotiaho, T., and Kulmala, M.: Sulfuric acid and OH concentrations in a boreal forest site, Atmos. Chem. Phys., 9, 7435-7448, doi:10.5194/acp-9-7435-2009, 2009.

Meusel et al 2016. = Meusel, H., Kuhn, U., Reiffs, A., Mallik, C., Harder, H., Martinez, M., Schuladen, J., Bohn, B., Parchatka, U., Crowley, J. N., Fischer, H., Tomsche, L., Novelli, A., Hoffmann, T., Janssen, R. H. H., Hartogensis, O., Pikridas, M., Vrekoussis, M., Bourtsoukidis, E., Weber, B., Lelieveld, J., Williams, J., Pöschl, U., Cheng, Y., and Su, H.: Daytime formation of nitrous acid at a coastal remote site in Cyprus indicating a common ground source of atmospheric HONO and NO, Atmos. Chem. Phys., 16, 14475-14493, doi:10.5194/acp-16-14475-2016, 2016.

Hellén et al. 2018 = Hellén, H., Praplan, A. P., Tykkä, T., Ylivinkka, I., Vakkari, V., Bäck, J., Petäjä, T., Kulmala, M., and Hakola, H.: Long-term measurements of volatile organic compounds highlight the importance of sesquiterpenes for the atmospheric chemistry of a boreal forest, Atmos. Chem. Phys., 18, 13839-13863, doi:10.5194/acp-18-13839-2018, 2018.

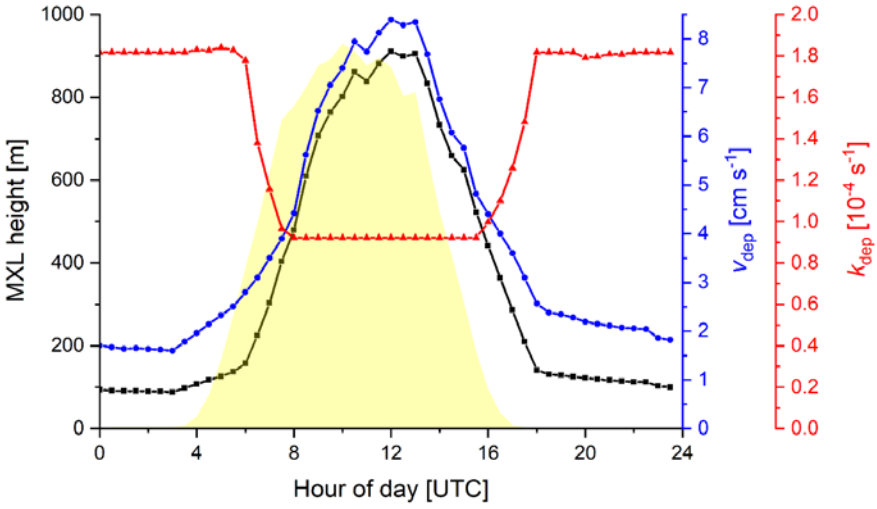

Figure S1: Diel profile of mixing layer (MXL) height (average of lidar and ERA Interim data) together with pyruvic acid deposition velocity (v_{dep}) and calculated deposition loss rate (k_{dep}) for the IBAIRN campaign.

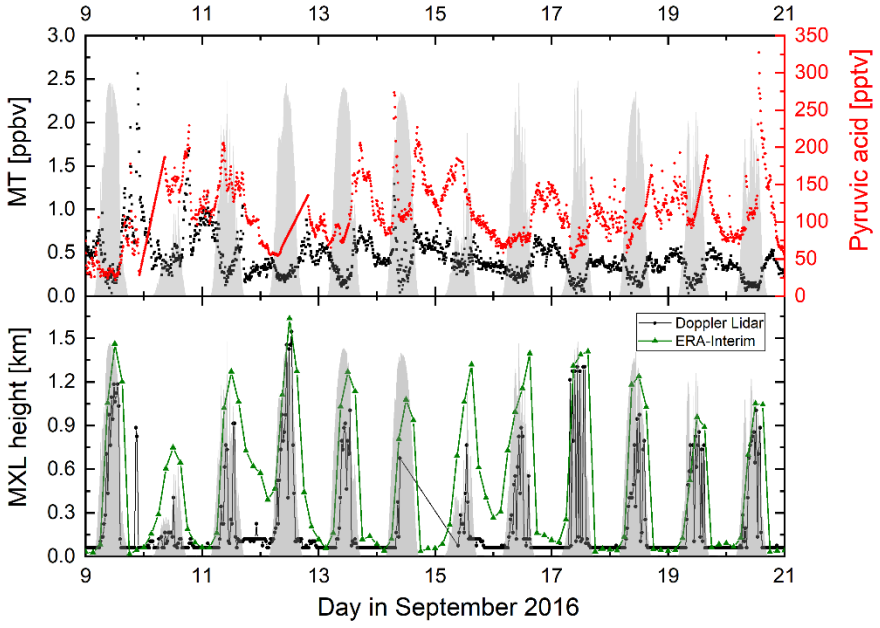

Figure S2: Upper panel: mixing ratios of MT and pyruvic acid along with the relative pyruvic acid photolysis rate (unitless, in grey) during the IBAIRN campaign. Lower panel: MXL height from a Doppler lidar and from ERA-Interim reanalysis.

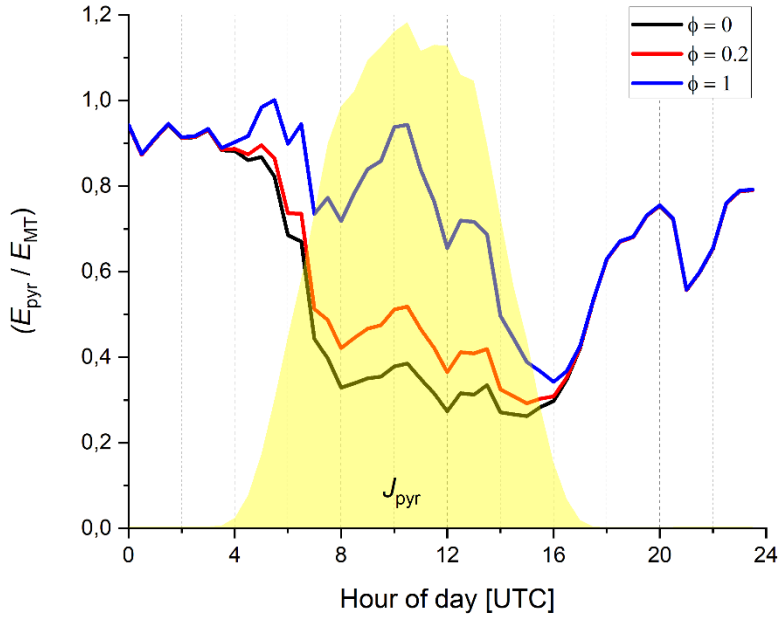

Figure S3: Diel variation in the emission rate of pyruvic acid relative to MT for different quantum yields (ϕ = 0, 0.2 and 1) along with the relative photolyss rate constant for pyruvic acid (J_{pyr}, shaded yellow).

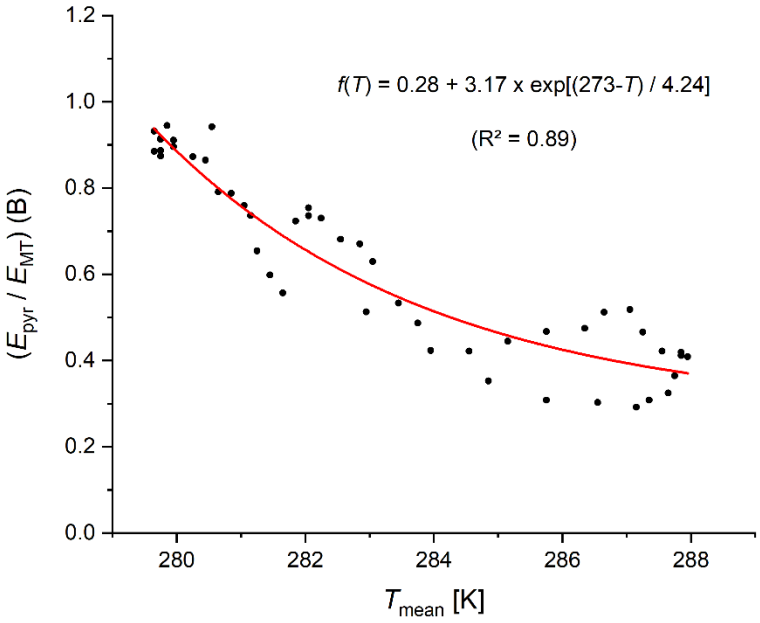

Figure S4: Temperature dependence of the emission ratio (E_{pyr} / E_{MT}) during the IBAIRN campaign.

Reaction scheme for pyruvic acid photolysis used in model scenario B:

Initial process:

$CH_3C(O)C(O)OH + h\nu$ (λ >340 nm)	$\rightarrow$	$CH_3COH^{\#} + CO_2$	$J_{PA} \times 0.75\ s^{-1}$
$CH_3C(O)C(O)OH + h\nu$ (λ <340 nm)	$\rightarrow$	$CH_3C(O)O_2 + HO_2 + CO_2$	$J_{PA} \times 0.25\ s^{-1}$

The factors 0.25 and 0.75 correspond to the actinic flux overlap with the PA-spectrum at λ < 340 nm and λ > 340 nm, respectively at local noon during the IBAIRN campaign. CH_3CO and HOCO are assumed to immediately react with O_2 to form $CH_3C(O)O_2$, HO_2 and CO_2.

Fate of the excited methyl hydroxy carbene ($CH_3COH^{\#}$):

$CH_3COH^{\#}$	$\rightarrow$	CH_3CHO	$1 \times 10^9 \times 0.20\ s^{-1}$
	$\rightarrow$	CH_2=CHOH	$1 \times 10^9 \times 0.10\ s^{-1}$
$CH_3COH^{\#} + M$	$\rightarrow$	$CH_3COH + M$	$1 \times 10^9 \times 0.7\ s^{-1}$

i.e. at one bar 20% of the initially formed $CH_3COH^{\#}$ form CH_3CHO and 10% form vinyl alcohol. This corresponds to the 2:1 ratio that (Samanta et al., 2021) report. The remaining 70% is stabilised by collisions. The overal rate constant ($1 \times 10^9\ s^{-1}$) is arbitrary (quasi-instantaneous).

Fate of the thermalised carbene (CH_3COH)

$CH_3COH + O_2$	$\rightarrow$	$CH_3C(O)O_2 + HO_2$	3×10^{-19} cm^3 molecule^{-1} s^{-1}
CH_3COH + HCOOH	$\rightarrow$	CH_3CHO + HCOOH	5×10^{-11} cm^3 molecule^{-1} s^{-1}
$CH_3COH + CH_3C(O)OH$	$\rightarrow$	$CH_3CHO + CH_3C(O)OH$	5×10^{-11} cm^3 molecule^{-1} s^{-1}

For a boundary layer with [HCOOH] + [$CH_3C(O)OH$] $\approx$ 0.7 ppbv and O_2 $\approx$ 20 % the loss rate constant are ~1.5 s^{-1} for reaction of CH_3COH with O_2 and 0.8 s^{-1} for reaction of CH_3COH with organic acids. For the conditions outlined above the yields (in percent, and per PA lost) are then:

CO_2	100
CH_3CHO	32
CH_2=CHOH	9
$CH_3C(O)O_2$	59

We do not consider photolysis of the carbene or reaction with H_2O, neither of which are competitive.

Samanta, B. R., Fernando, R., Rösch, D., Reisler, H., and Osborn, D. L.: Primary photodissociation mechanisms of pyruvic acid on S1: observation of methylhydroxycarbene and its chemical reaction in the gas phase, Phys. Chem. Chem. Phys., 23, 4107-4119, doi:10.1039/D0CP06424F, 2021.

Theoretical exploration of the reaction of pyruvic acid with CH_3COH

Due to the comparatively low concentration of pyruvic acid in the atmosphere, the reaction of $CH_3C(=O)COOH$ with CH_3COH is not expected to be important. However, as most experiments on pyruvic acid photolysis were often performed at sufficiently high concentrations of the acid to allow significant bimolecular reaction with the CH_3COH intermediate, it is worthwhile to briefly examine the reaction mechanism. As discussed below, we found the mechanism to be highly complex, and for some intermediates the chemistry is all but clear and may be unreliable at our level of theory. As such, the analysis here is intended mostly as an exploratory investigation.

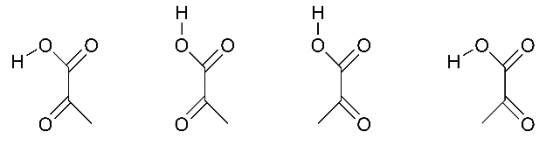

Pyruvic acid has several conformers, the most stable of which has the acidic H-atom pointing towards the non-acidic carbonyl group; this form constitutes ~97 % of the population at 298K (see inset above). Two other conformers exist with the H-bond internal to the carboxylic group, with a joined population of ~3 %. The fourth conformer, with no internal H-bond, has a negligible contribution to the population and is ignored in the remainder of this analysis.

The mechanism of the reaction of pyruvic acid with the CH_3COH carbene depends on the conformer of pyruvic acid that participates in the reactive encounter (see figure S5). For the conformers with an acidic H-bond, we find that the carboxylic acid group can catalyze without barrier the isomerization of *anti*-CH_3COH to CH_3CHO, similar to the mechanism already established for HCOOH. For both *syn*- and *anti*-CH_3COH, the acid-H-bonded pyruvic acid conformers can also form a strongly-bonded pre-reactive complex, and subsequently react with a negligible barrier to the $CH_3CH(OH)C=O)C(=O)CH_3$ adduct. We have not examined the subsequent chemistry of this adduct.

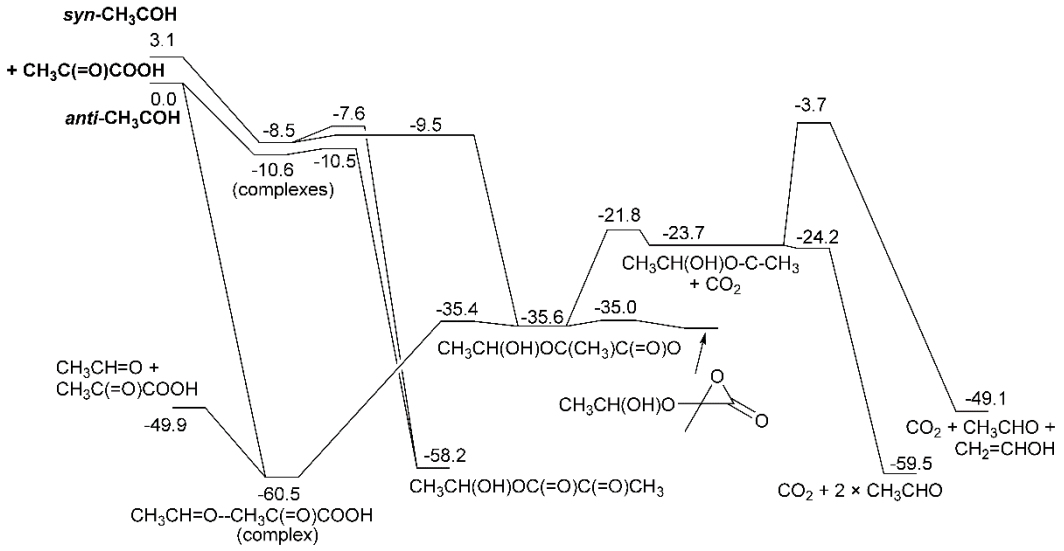

Figure S5: Potential energy surface (kcal mol^{-1}) of the reaction of CH_3COH with pyruvic acid, at the CCSD(T)//M06-2X-D3 level of theory. This surface should be considered as preliminary only.

The most stable pyruvic acid conformer, with an internal carbonyl H-bond, can form strongly bonded pre-reaction complexes with both *syn*- and *anti*-CH_3COH. The complex with *anti*-CH_3COH rearranges with a negligible barrier to pyruvic acid + CH_3CHO, i.e. it represents a second catalytic conversion channel for *anti*-CH_3COH to CH_3CHO. In contrast, for *syn*-CH_3COH, we found that the $CH_3CH(OH)OC(CH_3)C(O)O$ adduct is formed instead. At our level of theory, CCSD(T)//M06-2X-D3, this latter adduct has an unusual closed-shell wavefunction; no singlet biradical structure could be found using broken symmetry SCF/DFT. According to our results this intermediate can undergo reversible ring closure over a very low barrier, ≤ 1 kcal mol^{-1}, forming an iso-energetic epoxide. Depending on the relative orientation of the substituents, it can also undergo near-barrierless H-migration, regenerating pyruvic acid with a CH_3CHO co-product. CO_2 elimination has a higher barrier of 14 kcal mol^{-1}, forming a $C_4H_8O_2$ intermediate $CH_3CH(OH)OCCH_3$ (a carbene comparable to the $HOCCH_3$ reactant) that readily disproportionates to 2 CH_3CHO, or can rearrange to CH_3CHO + CH_2=CHOH after passing a high barrier. We were unable to find a pathway forming biradical species CH_3CO + CH_3CHOH or a rearrangement to the more stable $CH_3C(=O)CH(OH)CH_3$.

These calculations are far from conclusive to elucidate the products formed in the pyruvic acid + CH_3COH reaction. The strongly exothermic capture and complexation reactions followed by (near-)barrierless fragmentation or adduct formation suggests that the branching in the initial reaction pathways are strongly influenced by the dynamics of the reactants' approach,

and may not be well-described using traditional statistical methods. Also, the $CH_3CH(OH)OC(CH_3)C(O)O$ adduct seems to defy characterization at lower levels of quantum chemical theory, and we consider it likely that the wavefunction, and hence all subsequent chemistry, is still poorly represented at our chosen level of theory. Finally, while it is clear that the reaction of pyruvic acid + CH_3COH must be very fast and hence will play a critical role in many of the photolysis experiments, it is hard to reconcile the current potential energy surface with the product observations, such as those by Samanta et al. (2021) which observed a sufficiently stable $C_4H_8O_2$ product as well as CH_2=CHOH formation. The catalyzed isomerisation of CH_3COH to CH_3CHO, on the other hand, seems a recurrent reaction pattern. The current calculations indicate that further theoretical and experimental work is needed to fully explain all pyruvic acid photolysis experiment observations. As the reaction between the carbene and pyruvic acid is of low importance in the atmosphere, we did not pursue this further at this time.

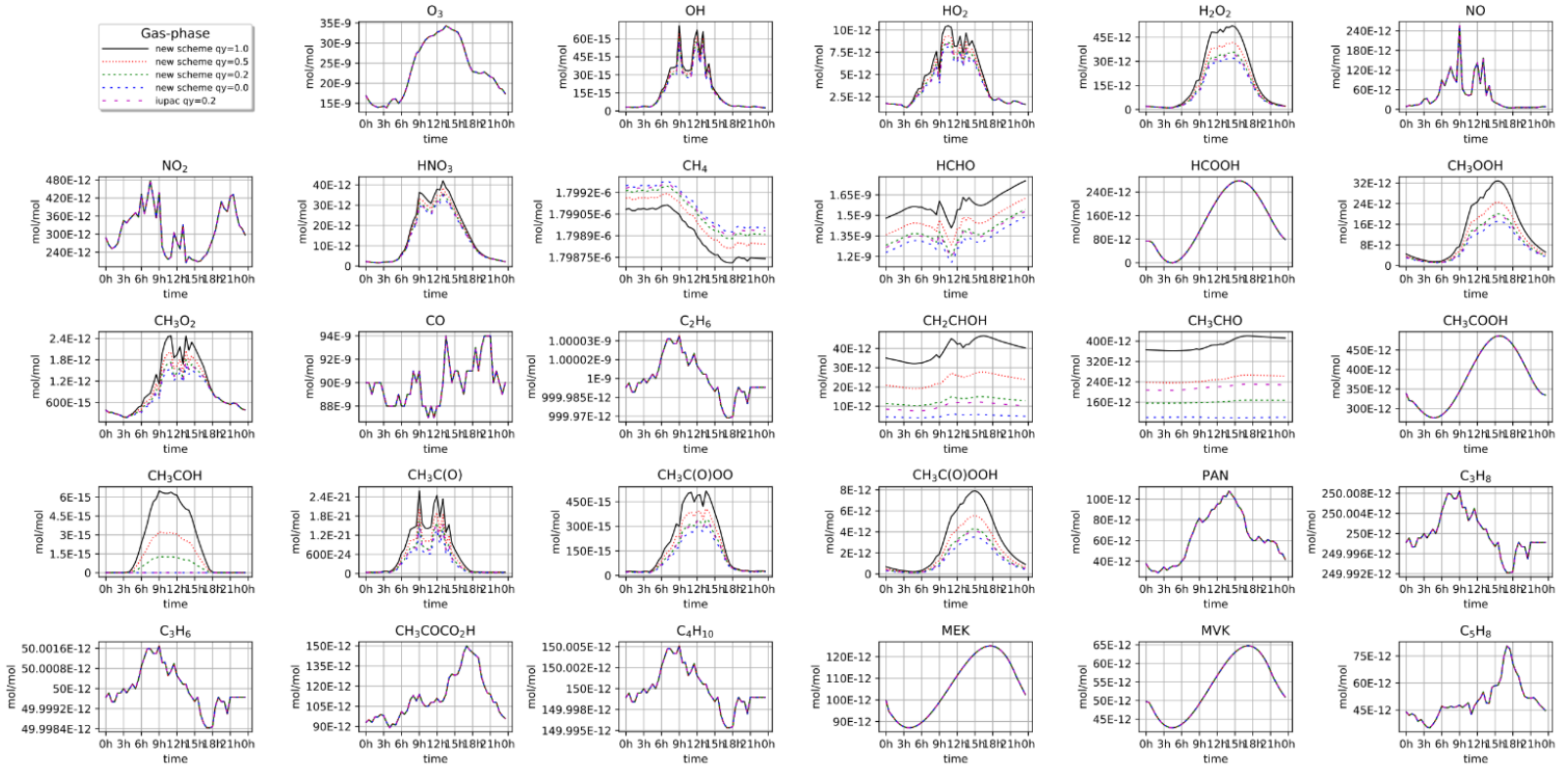

Figure S6. Modelled impact of pyruvic acid photolysis on the mixing ratios of various trace gases during IBAIRN. For trace gases that were constrained (e.g. PAN) the choice of scenario has no impact on mixing ratios.